ELSEVIER

Journal of Nuclear Materials 295 (2001) 179–188

journal of nuclear materials

www.elsevier.nl/locate/jnucmat

Atomic displacement cascade distributions in iron

A. Souidi [a], M. Hou [b,*], C.S. Becquart [c], C. Domain [d]

[a] *Centre Universitaire de Saida, BP138, En-nasr, Saida 20000, Algeria*

[b] *Physique des Solides Irradiés, Université Libre de Bruxelles, Bd du Triomphe, 50 Ave Franklin Roosevelt, CP234, B-1050 Brussels, Belgium*

[c] *Laboratoire de Métalurgie Physique et Génie des Matériaux, UMR 8517, Université Lille-1, F-59655 Villeneuve d'Ascq cedex, France*

[d] *EDF-DER Département EMA, Les renardières, F-77818 Moret sur Loing cedex, France*

Received 27 October 2000; accepted 19 March 2001

Abstract

Full molecular dynamics (MD) and its binary collision approximation (BCA) are used in a complementary way in order to study displacement cascade distributions in iron. Frenkel pair distributions are particularly narrow and symmetrical. They are thus well described by their first moment. Therefore, quantitative estimates by MD are possible. The comparison between the dependence of Frenkel pair production on primary energy predicted by both computational techniques suggests a post-cascade recombination model. Its physical grounds are discussed. The variability *between* spatial distributions of individual cascades is particularly large as a consequence of instability, which takes place in the early stage of the cascade development. The subsequent loss of correlation with initial conditions is statistically demonstrated on the basis of BCA simulations of 5000–15 000 cascades. Sufficient statistics can be reached by MD in order to characterise spatial distributions *within* cascades. It comes out of systematic comparison between MD and its BCA that, after the ballistic phase, the spatial extent of both vacancies and interstitials tends to increase. This phenomenon correlates with atomic mixing in the cascade core. This mixing is not predicted in the BCA. It is suggested to be responsible for the fragmentation of vacancy clusters formed during the ballistic phase of the cascades.

PACS: 63.43Bn; 6180Az; 6182Bg

1. Introduction

Atomic collision cascades subsequent to the neutron irradiation of materials represent the primary stage in radiation damage leading to macroscopic changes in the mechanical properties of materials. The development of these collision cascades and the damage resulting from the generation of energetic 'primary knock-on atoms' (PKAs) displaced from a bulk lattice site motivate extensive efforts in view of identifying and predicting the time evolution of mechanical properties of neutron irradiated materials [1–4].

Different theoretical approaches are available which developed simultaneously. The integral equation formalism [5–8] represents a major breakthrough in predicting spatial distributions resulting from continuous slowing down. Similar properties were also obtained by numerically solving the equations of motion of all cascade particles in a solid, using a binary collision approximation (BCA) [9,10]. The method was extended to the study of individual cascades as generated by a single PKA [11]. Solving the equations of motion in an individual cascade without using the BCA was achieved early [1,12–14]. This is full molecular dynamics (MD) which is nowadays a most commonly used method. Each of these methods is based on specific models that differ from each other. The integral equation was solved analytically with simple collision cross-sections for structureless materials. Lattice effects are extensively commented in the literature and a fundamental review may be found in [15]. The limitations of the BCA are extensively discussed as well.

* Corresponding author.
E-mail address: mhou@ulb.ac.be (M. Hou).

0022-3115/01/$ - see front matter
PII: S0022-3115(01)00556-6

The usual, though not general, neglect of interactions between moving particles when applying the BCA was pointed out early [16] (a noticeable exception is available in [17], where the BCA is used between moving atoms as well). The atomic interaction potentials represent the bottom of all models. An extensive early discussion may be found in [18]. Pair potentials used in the BCA are reviewed more recently [17,19]. A thorough discussion of the second moment tight binding and EAM potentials for MD simulations in iron is given in [20].

Much understanding may be expected from the comparison between different models as well as from measuring the effect of an approximation. Such an approach is only sparsely used in radiation damage studies. It is adopted as a basis of the discussion in the present work. Several issues will be emphasised by comparing full MD to the BCA predictions, which do not appear with one of these models independently.

The comparison between the time dependencies of recoil frequencies obtained by full MD and with the BCA is useful to fix the energy parameters inherent to the BCA and to identify their physical origin. This is done in [21] as briefly discussed in Section 2.2. It however does not necessarily warrant a full correspondence between both models. Indeed, such a comparison provides information neither about spatial correlations nor about atomic rearrangements at thermal energies, which may take place before the system comes to rest. Spatial damage distributions were found particularly broad as a consequence of an instability in the early stage of the cascade development, which initiates from stochastic thermal fluctuations [22]. A loss of correlation with other initial conditions is evidenced. The instability is the main factor determining spatial distributions but this does not exclude the contribution of other factors that will be discussed below, comparing MD and BCA predictions.

As a first example where the combined MD and BCA approach is useful, we shall discuss an apparent discrepancy found in [23] between the mean numbers of stable Frenkel pairs predicted by full MD and with the so-called NRT model [24]. The latter is based on the BCA. We shall show in Section 3 how to understand and reduce this discrepancy. A simple realistic model will be suggested for post-cascade atomic rearrangements involving spatial correlations. Spatial point defect distributions will then be discussed, again on the basis of comparisons between MD and BCA predictions. Such comparisons are the most useful to discuss spatial point defect correlations within individual cascades for which MD allows sufficient statistics to be reached. Statistical distributions *between* cascades will be discussed in Section 4, while Section 5 is devoted to spatial correlations *within* cascades.

We use displacement cascades in iron as a generic case study which ought to be valid for other crystalline and polycrystalline solids.

2. Atomic scale models

2.1. Full MD

Full MD has the advantage to model the time evolution of a box of atoms as a whole. It may be viewed as a method of solving numerically and stepwise in time a large set of coupled simultaneous equations of motion and suitable algorithms allow the computer time required to be made, therefore only linearly growing with the number of particles involved. In addition, despite the simultaneous character of the interaction between all considered particles, MD codes can be efficiently parallelised [25].

The MD code we use, DYMOKA, is a slightly modified version of CDCMD [26]: a user oriented code developed to perform Metropolis Monte Carlo and classical MD modelling.

The Newton equations of motion are integrated using a fifth-order gear predictor–corrector algorithm. The neighbour search is done through a linked cell method combined with a Verlet list [27]. This makes the code fully linear with the number of atoms. The interatomic potentials are tabulated and the interpolation of the potential tables is made through a fifth-order Lagrange polynomial. In this work, we used the EAM potential developed in [28].

In order to simulate displacement cascades, the following commonly used approximations are made. The effect of electron excitation is ignored. No damping forces are applied to the boundary atoms. Periodic boundary conditions (PBC) are used with a choice of the simulation box size depending upon the energy of the PKA.

At the beginning of the simulation, the system of particles is let to equilibrate for 5 ps. Most of the time, the temperature of the irradiated iron is set to 600 K, which is representative of reactor vessels working conditions. When the lattice is at thermal equilibrium, one atom, the PKA is given a momentum corresponding to energies from 1 to 30 keV. The actual timestep is 'manually' adapted to the PKA velocity, and it can be as low as 10^{-17} s. As soon as the extreme collisions are over, a much longer timestep is adequate, i.e., 10^{-16}–10^{-15} s. More detail on the procedure can be found in [20].

2.2. The BCA of MD

Accumulating statistics over large samples of collision cascades is nowadays still unpractical in the energy

ranges of interest for radiation damage studies. This drawback is drastically reduced by the BCA of MD, at the expense of an approximate treatment of multiple simultaneous interactions. The BCA is several orders of magnitude less time consuming than MD and it therefore allows reasonably significant statistics in case of widespread statistical distributions. However, since the consequences of the approximate treatment of simultaneous events are not all fully identified, BCA needs to be grounded, for instance on MD results, as much as possible. On the other hand, the BCA is inappropriate to describe the evolution of a system close to thermal equilibrium while MD is ideally suited therefore. Advantage is taken from this difference in the present discussion and a comparison between BCA and MD results will allow information to be provided about the magnitude of post-ballistic effects.

The Marlowe program (version 14c) is used in what follows. A huge variety of displacement models are available. They are described through an extensive literature, probably starting in 1963. A basic reference is given in [29]. Collision cascades are modelled as sequences of binary encounters between which atoms move freely along their scattering asymptotes. Individual collisions are governed by pair potentials that may have an attractive component [30]. A series of potential functions is available in the Marlowe package and others may be implemented. The potential function is used to estimate the scattering angle and the time integral in each binary collision. Integration is achieved by means of a quadrature whose number of nodes may be tuned. In such a way, the scattered and recoil atomic momenta, as well as the exit asymptote positions, are calculated. In the present work, the pair potential suggested in [31] is generally used and occasionally, when mentioned, the Molière approximation to the Thomas Fermi potential [32]. According to the notations in [33] the former model potential will be noted AMLJ. The reason to use the AMLJ potential preferentially is that it compares well with the repulsive branch of the EAM potential used in the present MD modelling at small separation distances. Electron excitations may be modelled by means of the quasi-elastic approximation [34], according to Lindhard's theory [35], or both. Other models may be used. However, in view of comparisons with the full MD model described above, this possibility will not be used in the present study. The binary collisions are chronologically ordered so that time represents the driving parameter in the cascade development. The number of collisions undergone by the moving atoms is limited by a maximum impact parameter value selected by the user.

The dynamics of the atomic ballistic phase have already been discussed in the case of low energy collision cascades in copper and gold [21]. In that work, a comparison between the MD and the BCA predictions of the mean number of moving atoms as functions of time was carried on. Except for the BCA itself, the models were made as close as possible. In this respect, the repulsive branches of both model potentials were identical, although no attractive potential component was considered in the BCA.

Provided lattice atoms are considered to be bound to their lattice site with a binding energy equal to the material cohesive energy, in elemental metals, the MD and the BCA predicted most similar cascade dynamics. The agreement was found to be excellent for all atoms moving with total energies as low as 0.5 eV. In replacement collisions; however, since both the initial and final situations are similar (one moving interstitial and one identical lattice atom), the binding energy to a lattice site was considered as much reduced as compared to the cohesive energy, and a value of 0.2 eV was suggested. This order of magnitude is consistent with the comparison between various models made in [15].

In the present study, for iron, we use a maximal impact parameter a little smaller than the first neighbour distance. Energy parameters are available in various models for the binding of atoms to their lattice site and to cutoff their trajectories. In what follows, the binding energy of the atoms to their lattice sites is considered constant and direction independent. It is fitted to the cohesive energy in the matrix, as suggested by the previous comparison between MD and its BCA mentioned above [21]. The binding energy in replacement sequences is taken as 0.2 eV, independently of the sequence direction.

2.3. Characterisation of spatial point defect distributions

Component analysis is an efficient technique to uniquely associate an ellipsoid to each individual displacement cascade, which accounts for its spatial extension and its morphology on the basis of its intrinsic characteristics [11]. It is thus useful for making comparisons between cascades. The information provided by this method is the direction of three orthogonal axes that are associated to the spatial point defect distribution and the variance of this distribution projected onto them. The major axis has the direction maximising the variance, the second maximises the variance of the distribution projected onto a plane perpendicular to the first and the third one has the direction minimising this variance.

In order to determine these directions, one looks for the unitary vector $\mathbf{u}$ such that

$$S^2 = \sum_{k=1}^{n} |f_k|^2 = (\mathbf{u}\cdot\mathbf{r}_k)^2 = \mathbf{uRu} \quad \text{with } \mathbf{R} = \sum_{k=1}^{n} \mathbf{r}_{ki}\mathbf{r}_{kj} \;\; i,j = 1,3 \tag{1}$$

is maximal. f_k is the projection of the position vector $\mathbf{r}_k$ of point k on the major axis. $\mathbf{R}$ is proportional to the covariance matrix. When S^2 is maximum, its derivative with respect to $\mathbf{u}$ is zero and this implies

$$\mathbf{Ru} = \alpha^2\mathbf{u}; \tag{2}$$

$\mathbf{u}$ is thus an eigenvector of $\mathbf{R}$. Comparing (1) and (2) shows that S^2 is associated to the eigenvalue α^2. The second axis direction $\mathbf{v}$ is found such that $\mathbf{vRv}$ is maximal with the constraint $\mathbf{v}\cdot\mathbf{u} = \mathbf{0}$. $\mathbf{v}$ is also shown to be an eigenvector of $\mathbf{R}$ associated to an eigenvalue β^2. β^2 is the variance of the distribution projected on $\mathbf{v}$. The same reasoning applies to the third direction $\mathbf{w}$ with the eigenvalue γ^2. These directions are parallel to the directions of the eigenvectors of the covariance matrix of the point defect distributions and the associated eigenvalues are the variances of the distribution projected onto the directions of the eigenvectors. The problem is thus limited to the diagonalisation of a 3×3 symmetrical real and positive matrix, which is quite straightforward.

The eigenvectors and eigenvalues naturally define an ellipsoid associated with each cloud of point defects whose axes lengths are given by the standard deviation of the distributions projected in the directions of the eigenvectors. These ellipsoids define the cascade cores. In what follows, and for simplicity, each core volume will be considered as representative of one displacement cascade. Volume distributions will be constructed. Similarly, the anisotropy of each cascade core will be measured as the ratio between the lengths of the axes maximising and minimising the projected distribution variance. A more sophisticated approach is developed in [36], which allows to account for cascade inhomogeneities and subcascade formation, thus possibly associating more than one ellipsoid per cascade, but this is not necessary for the present discussion.

Point defect distributions within cascades will be mainly discussed in terms of pair correlation functions. Standard definitions are used to characterise inner distributions of vacancies, of interstitials and closest vacancy–interstitial pairs.

3. Frenkel pairs

The variance of the Frenkel pair frequency distribution obtained both in the BCA and by MD is quite small when the PKA is initiated from a lattice site (the situation is different in case of external irradiation). These were already studied by several authors either analytically [37] or on the basis of BCA calculations in [9], including a discussion of the significant role of electronic excitation. This role is discarded in the present discussion. Owing to this predicted small variance, the mean number of Frenkel pairs produced by collision cascades can be determined accurately on the basis of limited samples. It was estimated in [9] that, in the case of copper, at 10 keV, a sample of 20 cascades should yield only to about 1% uncertainty in the value of the mean number of Frenkel pairs. This is qualitatively confirmed by the MD calculations performed here as well as those by [38]. In both works, 10–20 cascades were sufficient to limit the uncertainty to a few percent.

At this stage, the important point is that, whatever the Frenkel pair production model, the predicted variance is small and reasonable statistics can nowadays be reached by MD within limited computer times for several 10 keV cascades. The apparent discrepancy between MD and its BCA, mentioned in the introduction, is now studied by comparing both approaches.

In full MD, a Frenkel pair is considered to be stable if it survives a 'long' time (5 ps) as compared to the cascade characteristic lifetime (of the order of 1 ps), though quite short as compared to the characteristic diffusion time at room temperature.

The physics involved in Frenkel pair production is not yet fully understood and, in the BCA, a displacement threshold is often considered with a magnitude of several 10 eV [39], considering that an atom recoiling with less energy would spontaneously recombine. Such a parameter is however not quite convenient as it is strongly direction dependent. Evidence for this direction dependence is available, from both computer simulation (see, e.g. [40]) and direct experiment (see, e.g. [41]). An alternative, whose physical grounds are clearer, is to account for an instability volume [42]. A Frenkel pair is considered to be stable if and only if its vacancy–interstitial separation distance is larger than this unstability, or, recombination radius. In such a scheme, recombination is considered as athermal and not dependent on direction. It is also not a collisional process. MD evidence for such an athermal process is given in [43]. In this scheme, the recombination process involves more than one atom (the interstitial) and one atomic site (the vacancy). It implies local collective rearrangement.

Vacancy–interstitial pair distribution functions can be constructed in the BCA with good statistics and the value of a suitable recombination radius can be deduced by matching these distribution functions to the number of stable Frenkel pairs computed by MD. This is done according to the procedure illustrated in Fig. 1 for iron. In this figure, the number of Frenkel pairs obtained at 600 K by MD is represented as a function of the PKA energy and compared with the BCA results. These are obtained with a negligibly small displacement threshold value and different recombination radii, noted r_c. Typically, the energy displacement threshold is taken smaller than the binding energy of the atoms to their lattice site. This way, it plays no significant role in the cascade development. As seen in Fig. 1, the BCA results obtained with the AMLJ potential are in good overall agreement

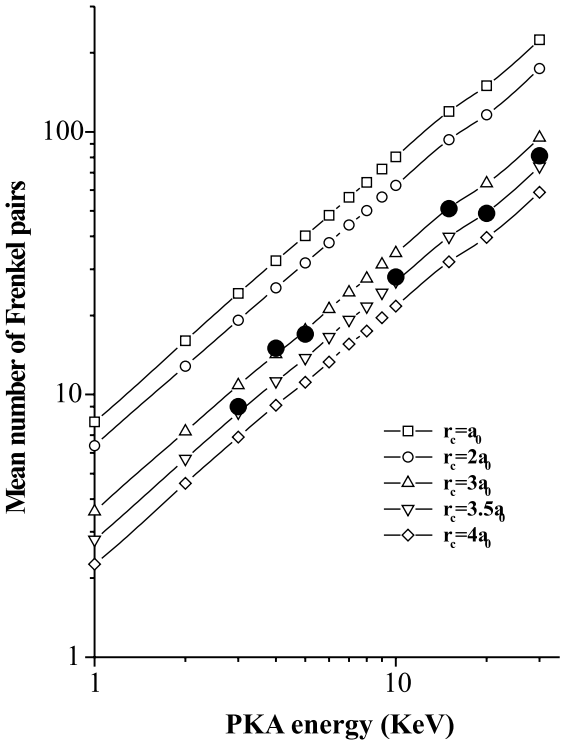

Fig. 1. Mean number of Frenkel pairs produced as a function of the PKA initial energy as obtained by MD (filled circles) and in the BCA, accounting for a spontaneous recombination radius, r_c. BCA results are shown for $a_0 < r_c < 4a_0$, where a_0 is the lattice distance in iron. MD and its BCA lead to quantitatively similar dependencies when $3a_0 < r_c < 3.5a_0$.

with MD for $3a_0 < r_c < 3.5a_0$. With the Molière potential, the best matching was found for $4.5a_0 < r_c < 5a_0$ [44].

Similar overall agreement, over the same energy range, is found with other published MD data [23] in the case of copper, titanium and nickel, using, in the BCA, a Molière potential. The appropriate recombination radii turn out to be of the same order and not significantly PKA-energy dependent in the range investigated. In the case of copper, a recombination radius of $2.5a_0$ provides an excellent agreement between BCA and MD. This separation distance is found to be equal to that at which the vacancy–interstitial binding energy tends to vanish. It is thus tempting to correlate the recombination radius with this vacancy–interstitial distance. Such a correlation is however only qualitative since it neglects the excitation state of the cascade area and the subsequent phenomena.

In the case of iron, the recombination radius found in Fig. 1 with the Molière potential is in agreement with experimental estimates by electron irradiation of a perfect iron crystal [45]. The former is somewhat larger than the distance at which the vacancy–interstitial binding energy is found to vanish with the potential used in the displacement cascade MD simulations. We found this distance to be $1.7a_0$, where a_0 is the 0 K equilibrium lattice parameter. It thus appears that the maximal binding distance between a vacancy and an interstitial is not sufficient to account for recombination. Therefore, in order to bring further understanding, a more detailed study of the cascade development as modelled by full MD and in its BCA is necessary. This is the subject of Section 5. The following section discusses the stochastic properties of collision cascades and their consequences.

4. Statistical distributions between cascades

Figs. 2(a) and (b) display the final configurations of the residual vacancies and interstitials at the end of two different 20 keV collision cascades modelled by MD at 600 K with different initial conditions. They were both calculated with a PKA directed toward the same $\langle 1\,3\,5\rangle$ direction. The influence of the PKA direction was already examined by MD in [46] and the results support the view that the $\langle 1\,3\,5\rangle$ initial direction should provide cascade distributions typical of most occurring events. The differences observed in Fig. 2 are typical of all cascades investigated by MD. The most important point to notice is that these cascades differ only by the random number used in thermalising the simulation box at 600 K. The only difference when launching the PKA at different times is therefore the initial instantaneous thermal phase space configuration. It is obvious at first glance that the final vacancy and interstitial configurations depend substantially on the initial thermal configuration, hence inducing significant configurational variance in the final state of the system.

A similar experiment can be repeated in the BCA. In the Marlowe model, lattice atoms may be considered as initially displaced at random within a Gaussian distribution. In this work, we determine its variance from the Debye temperature. This is consistent with the Einstein model of thermal vibrations. Since, within the Marlowe model, target atoms are always considered at rest, the initial phase space configuration reduces to the atomic position coordinates. 20 keV cascades were initialised in a $\langle 1\,3\,5\rangle$ direction at 600 K and a post-cascade recombination radius of 3.5 lattice units is used, such that the mean number of Frenkel pairs is the same as obtained by MD (see Fig. 1). The results are shown in Figs. 2(c) and (d) for cascades representative of the whole set investigated. Similar trends are found with both simulation models and the variance in the final configuration is found qualitatively as significant as in the case of full MD. It is shown in [22] that this variance reflects an instability, which develops in the early stage of the cascade.

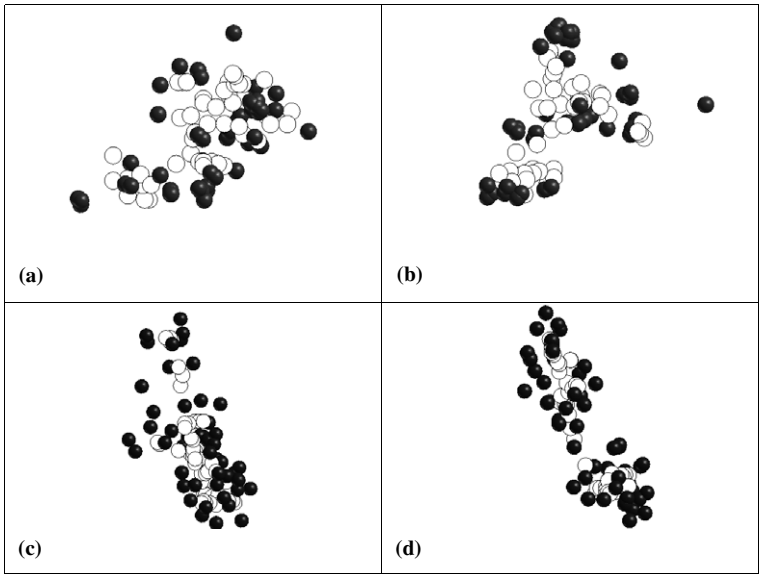

Fig. 2. Final cascade induced point defect configurations obtained by MD (a,b) and in the BCA (c,d). The temperature is 600 K. Except for the thermal configurations, the initial conditions are identical. The PKA is a lattice atom with a kinetic initial energy of 20 keV and momentum pointing in the $\langle 1\,3\,5\rangle$ direction. In the BCA, a recombination radius of $3.5a_0$ is chosen, according to the results in Fig. 1 at 20 keV.

Visual inspection of such final configurations does not allow to distinguish between cascades generated by full MD or in its BCA. Vacancies tend to cluster into a core surrounded by the interstitials, consistently with the pioneering schematic picture of Brinkman [47]. Subcascade formation is found to take place with some significant probability. Since all other initial conditions are identical, the spatial configurations of displacement cascades, and thus of their volumes, point defect densities, and morphologies (including subcascade formation) only result from uncorrelated thermal configurations. Hence, they only can be characterised by statistical distributions. It is shown below that the first moment of these distributions does not provide much information about them.

In order to characterise the cascade size, the component analysis is used as described above. Ellipsoids are constructed that define the vacancy cascade cores. Statistics is accumulated in the BCA over several thousand cascades with the AMLJ potential. A recombination radius is again chosen so as to match the mean number of Frenkel pairs obtained by MD.

Typical core volume distributions of 20 keV cascades are given in Fig. 3(a). An anisotropy factor is defined as $\eta = \alpha/\gamma - 1$, where α and γ are the major and minor axes lengths of the ellipsoid, respectively. An anisotropy factor distribution is shown in Fig. 3(b). The temperature is 600 K. In one series of simulations, 5000 cascades are generated by PKAs starting from the same lattice site in the same $\langle 1\,3\,5\rangle$ direction. The only difference in initial conditions from one cascade to another is the thermal configuration. A second series of 15 000 cascades, generated by selecting the PKA directions at random and isotropically, provides another pair of core volume and anisotropy factor distributions. These are shown in Fig. 3 to be indistinguishable from the former, demonstrating that the correlation with the initial primary direction is lost. Both distributions are pronouncedly skewed toward high values (the tails of the distributions are cutoff for the purpose of drawing) and subsequently, the most probable and mean values differ significantly. Similar distributions are found for other PKA energies.

Besides the loss of correlation, one essential point at this stage is that all distributions are quite broad and the widths relative to modal values are over 100% in contrast with the Frenkel pair frequency distributions.

The huge variability found is the consequence of the thermal displacements only. The root mean square thermal vibration amplitude is less than 0.1 Å at 600 K. This was shown in [22] by both MD and its BCA to be the consequence of a well-known diverging evolution (see, e.g. [48] or [49]) in the early stage of the cascade development. It is this divergence which is at the origin of the loss of correlation evidenced by Fig. 3. As a consequence, the final cascade configurations are unpredictable and they can only be characterised in terms of distributions.

MD cannot reach similar statistics as possible in the BCA, unfortunately. The individual MD results ob-

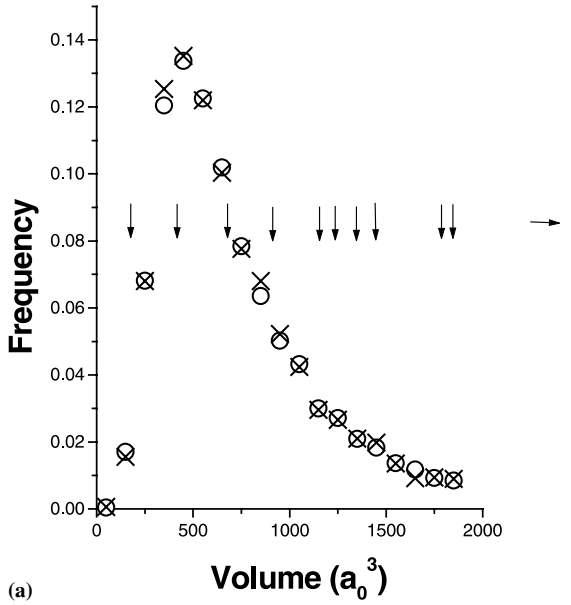

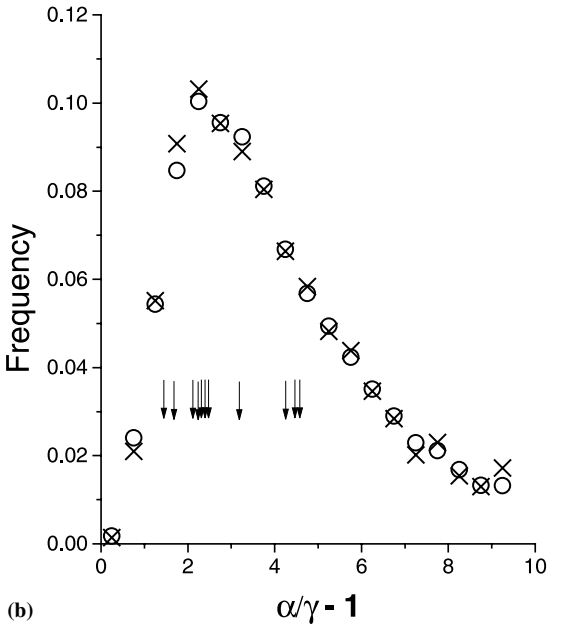

Fig. 3. (a) Vacancy cascade core volume distributions as obtained in the BCA with 20 keV PKAs directed toward the ⟨1 3 5⟩ directions (crosses) and with incident directions selected isotropically and at random (circles). Statistics is accumulated over 5000 cascades in the former case and 15 000 in the latter. (b) Anisotropy distributions corresponding to the same vacancy cascades as used in (a). Volumes estimated the same way and obtained by MD simulations are shown with vertical arrows. The horizontal arrow indicates an MD vacancy cascade volume which is larger than that represented in the figure.

tained by the same component analysis method as above are marked in Fig. 3. The individual results displayed are sufficient to conclude that the core volume distribution is broad as well. MD and the BCA seem to predict similarly widespread spatial vacancy and anisotropy factor distributions. The statistics over the limited number of available MD cascades is however not sufficient to draw any quantitative conclusion.

More details however can be emphasised by examining vacancy clusters inside the individual cascades. This is done for different PKA energies. A cluster is here defined as a group of vacancies having neighbouring vacancies at a distance smaller than or equal to the second neighbour distance.

The comparison is shown in Fig. 4. In the BCA, about 45% of the vacancies have no such close neighbours and are thus considered as isolated. Most similar results are obtained when the simulations are repeated with the Molière potential. With similar initial conditions for a 20 keV PKA, this number, as obtained by MD, is close to 70%. The tendency to cluster was found to be significantly potential dependent in [20], which would tend to prove that this characteristics of the damage is directly related to the equilibrium part of the potential. The modelling of the equilibrium part of the potential in the BCA is restricted to an amount of binding energy of the atoms to their lattice site taken

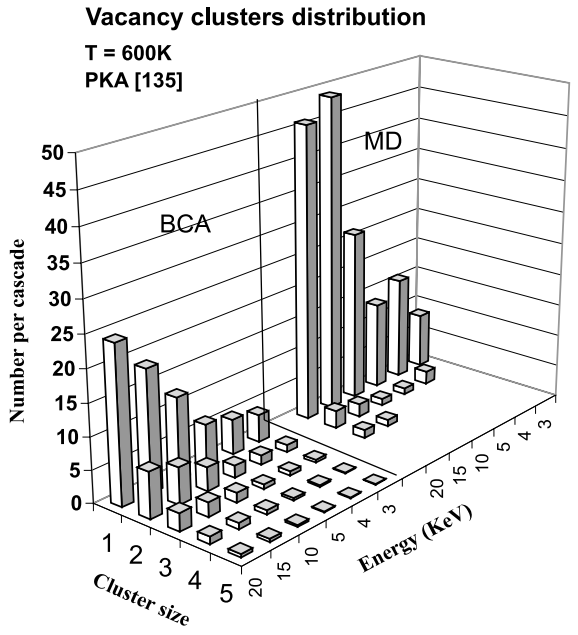

Fig. 4. Vacancy cluster distributions as obtained in the BCA and by MD for different PKA energies. The 'cluster size' represents the number of vacancies in one cluster. The temperature is 600 K and the PKA direction is parallel to the ⟨1 3 5⟩ crystal direction.

equal to the cohesive energy, which is equal to the equilibrium EAM value of the configuration energy. The results in Fig. 4 can thus only be considered as qualitative. An attempt is made in Section 5 to understand why MD cascade values may be larger than when estimated in the BCA.

The results in the present section are hampered by a lack of statistics. Reasonable statistics can however be reached by MD in spatial properties within cascades, which allow more quantitative comparison with the BCA. This is the approach used in the following section.

5. Statistical distributions within cascades

In what follows, we compare the vacancy–vacancy distance and the vacancy–interstitial distance pair correlation functions in MD and BCA cascades obtained starting with identical initial conditions. In the BCA, statistics is accumulated over one thousand cascades. Although less than 10 cascades could be modelled by full MD in each conditions considered, significant trends are found, which allow quantitative comparison.

A typical vacancy–vacancy pair correlation function, noted $g_{V\text{-}V}(r)$ is given in Fig. 5. The overall agreement is quite reasonable. It however appears that small vacancy–vacancy distances are more frequent in the BCA than predicted by MD while the situation is reversed at large distances. This means that, on the average, the vacancy separations are slightly smaller when predicted in the BCA than by full MD.

An additional relevant difference between MD and its BCA is found by a careful analysis of the first peak structure. This peak is composed of two channels: the first one corresponds to the first neighbour distance while the second one corresponds to the second neighbour distance. The BCA turns out to privilege first neighbouring vacancies while full MD privileges second neighbours. Second neighbour vacancies indeed induce smaller lattice relaxation in iron and the associated binding energy is accordingly larger (0.21 eV to be compared to 0.16 eV for first neighbour vacancies, as evaluated with the EAM potential used in this work), which makes them more probable. Such relaxation effects cannot be taken into account in the BCA.

Fig. 6 shows the vacancy–interstitial pair distance correlation function, noted $g_{V\text{-}I}(r)$. The sharp edge at small distances found with the BCA reflects the use of a sharp threshold recombination distance (a smoothly vanishing recombination probability with distance could have been somewhat more realistic). The amount of closer distance pairs found by full MD is negligible, showing that the recombination threshold distance used in the BCA is reasonable. A significant difference appears between full MD and its BCA. The BCA distribution is indeed narrower than the MD one and exhibits a peak at a smaller distance. Furthermore, the MD peak decays more slowly, while at the largest distances, frequencies are similar. This difference can be partly interpreted as a 'post-ballistic' effect. First, the simulations are achieved at rather high temperature (600 K), which contributes to shorten the length of replacement sequences and to promote thermal diffusion. In case of correlated thermal vibrations, re-

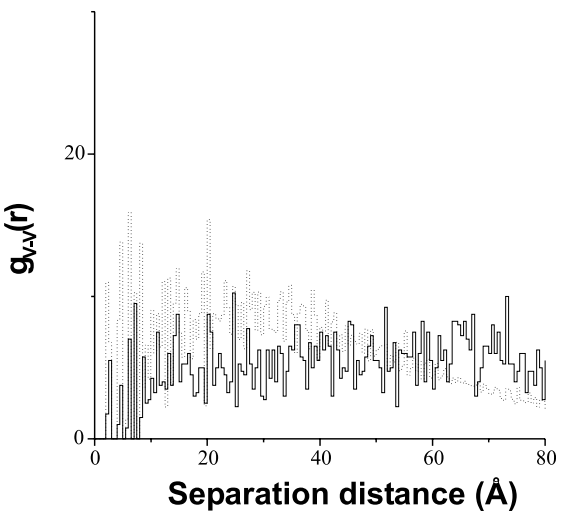

Fig. 5. Vacancy pair correlation functions obtained by MD (solid line) and in the BCA (dotted line). The PKA energy is 20 keV, the initial momenta are directed parallel to the ⟨1 3 5⟩ direction and the temperature is 600 K.

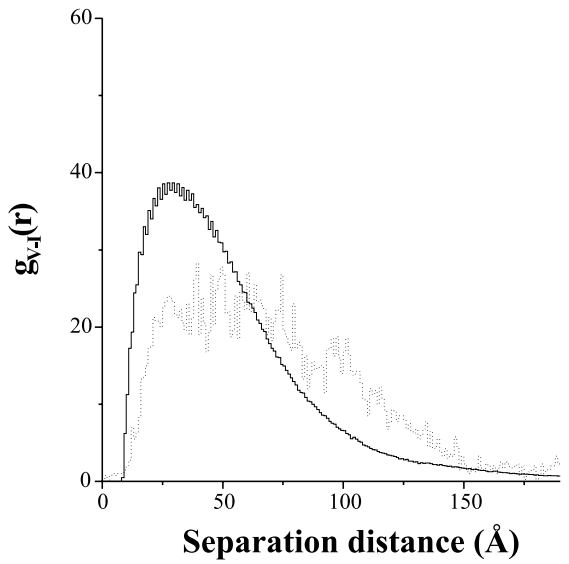

Fig. 6. Closest vacancy–interstitial pair correlation functions obtained by MD (dotted line) and in the BCA (solid line). The conditions are the same as in Fig. 5.

placement sequences may be longer in MD than in the BCA where such correlations, if any, are ignored. To check on this point, the BCA simulations were repeated at 0 K in order to increase artificially the length of replacement sequences. This only partially improves the matching with MD results. Therefore the replacement sequence length cannot explain the differences between MD and its BCA. On the other hand, the strong, though short lived, local energy gradient oriented toward the outside of the cascades induces a directional constraint on the thermal diffusion of cascade interstitials that aim at condensing them on 'cold' areas. This may explain the slower decay of the MD peak at intermediate distances. Since this thermal transport is short lived, the effect is only limited in space and does not affect the interstitials that are the most distant from the cascade core, hence the good agreement between MD and the BCA at large distances.

Another post-ballistic effect is the atomic mixing in the cascade core. Mixing is extensively studied, in particular in the case of metallic binary alloys, and a good deal of the MD simulations done is reviewed in [50]. Alloys are convenient therefore because mixing produces chemical disorder, which is easy to detect. Disorder however does not evidence the whole mixing which takes place during irradiation, since mixing between atoms of the same nature is not identified. In a computer simulation, it is however straightforward to single out every lattice site where an atom has been replaced by another, whatever its identity. This is done in the present work and the results shown in Fig. 7 clearly demonstrate the non-linear nature of the process. Indeed, the mean number of replacements found in the BCA is proportional to the PKA energy, as expected from a linear model. In contrast, a faster than linear dependence on the PKA energy is found by full MD. The present BCA model does not account for this non-linearity.

In addition to this non-linear dependence on the PKA energy, the replacement frequency measured by MD is more than twice that estimated in the BCA, even at the lowest PKA energies considered. This is the consequence of the rearrangements among the lattice sites resulting from the collective recombination process discussed in Section 3. This one is not accounted for in the BCA results of Fig. 7. In a dense cascade, recombination volumes overlap, leading to an overall mixing area, and the fraction of sites taking part in recombination in each recombination volume is hardly estimated. Therefore, a quantitative relation between the BCA and the MD results in Fig. 7 cannot be established and, at present stage, it is not possible to decide to which extent the non-linear behaviour found is due to a local increase of the recoil density or of the recombination radius.

Whatever the origin, the present model prediction difference may be related to the differences found in the spatial distributions of vacancies. It suggests that the more efficient mixing found by MD contributes to dissolve the vacancy clusters in individual cascades, hence increasing the number of isolated vacancies. Further investigation is however necessary to settle this point.

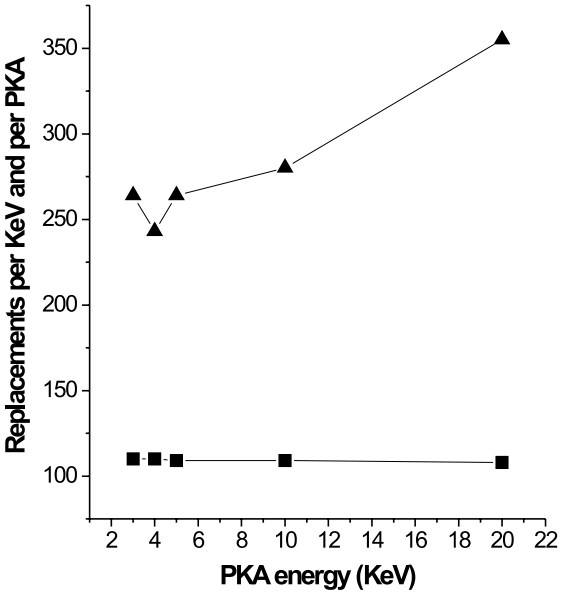

Fig. 7. Replacement frequencies as estimated at the end of the cascades by MD (triangles) and in the BCA (squares) as a function of the primary energy.

6. Conclusion

By comparing displacement cascades calculated by full MD and in its BCA, physical aspects of the cascade development could be emphasised. A simple recombination model was sufficient to make Frenkel pair frequency distributions consistent with each other. The comparison supports the suggestion of an instability volume within which spontaneous vacancy–interstitial recombination takes place. MD evidence for a recombination distance threshold comes out of the study of vacancy–interstitial pair correlation functions. The contribution of athermal recombination, however, could not be distinguished from other contributions to cascade mixing.

As already noticed elsewhere [20], the spatial extent of individual cascades is essentially governed by the early stage of their development. This early stage is dominated by an instability, which results in particularly broad and skewed statistical spatial distributions.

Cascade mixing is confirmed to be an increasing function of the PKA energy. One consequence is to

fragment the vacancy clusters formed during the ballistic phase of the cascades. The volume occupied by the interstitials is suggested to be enhanced by a short lived energy gradient toward the outside of the cascades. Hence, significant post-ballistic effects are detected and measured in point defect distributions within displacement cascades.

Full MD and its BCA thus appear to be complementary in characterising primary damage and the comparison between the predictions helps in evaluating the magnitude of post-ballistic effects.

Acknowledgements

Part of this work was performed under contract IUAP 4/10 with the Belgian Federal Government.

References

[1] J.B. Gibson, A.N. Goland, M. Milgram, G.H. Vineyard, Phys. Rev. 120 (1960) 1229.
[2] M.T. Robinson, in: Proceedings of the International Summerschool on the Fundamentals of Radiation Damage, Urbana, IL, August 1993.
[3] W.J. Phythian, R.E. Stoller, A.J.E. Foreman, A.F. Calder, D.J. Bacon, J. Nucl. Mater. 223 (1995) 245.
[4] R.S. Averback, T. Diaz de la Rubia, Solid State Phys. (1998) 281.
[5] G. Kinchin, R. Pease, Rep. Progr. Phys. 18 (1955) 1.
[6] M.T. Robinson, Philos. Mag. 12 (1965) 741.
[7] J. Lindhard, Mater. Fys. Medd. Dan. Vid. Selsk. 33 (10) (1968).
[8] K.B. Winterborn, P. Sigmund, J.B. Sanders, Mater. Fys. Medd. Dan. Vid. Selsk. 37 (14) (1970).
[9] M.T. Robinson, I. Torrens, Phys. Rev. B 9 (1974) 5008.
[10] M. Hou, Nucl. Instrum. and Meth. B 13 (1986) 331.
[11] M. Hou, Phys. Rev. B 31 (7) (1985) 4178.
[12] R.P. Webb, D.E. Harrison Jr., K.M. Barfoot, Nucl. Instrum. and Meth. B 7–8 (1985) 43.
[13] J.R. Beeler, in: S. Amelinckx, R. Gevers, J. Nihoul (Ed.), Radiation Effects Computer Experiments, North-Holland, Amsterdam, 1983.
[14] W.E. King, R. Benedek, J. Nucl. Mater. 117 (1983) 26.
[15] M.T. Robinson, in: R. Behrisch (Ed.), Sputtering by particle bombardment, Springer, Berlin, 1981.
[16] P. Sigmund, Appl. Phys. Lett. 25 (1974) 169.
[17] Y. Yamaura, Nucl. Instrum. and Meth. B 51 (1990) 407.
[18] P.C. Gehlen, J.R. Beeler Jr., R.I. Jaffee (Eds.), Interatomic Potentials and Simulation of Lattice Defects, Plenum, New York, 1972.
[19] W.G. Eckstein, Computer Simulation of Ion-Solid interactions, Springer, Berlin, 1991.
[20] C.S. Becquart, C. Domain, A. Legris, J.C. Van Duysen, J. Nucl. Mater. 280 (2000) 73.
[21] M. Hou, Z.-Y. Pan, Radiat. Effects 142 (1997) 483.
[22] M. Hou, A. Souidi, C.S. Becquart, J. Phys. C, in press.
[23] D.J. Bacon, A.F. Calder, F. Gao, V.G. Kapinos, S.J. Wooding, Nucl. Instrum. and Meth. B 102 (1995) 37.
[24] M.J. Norgett, M.T. Robinson, I.M. Torrens, Nucl. Eng. Design 33 (1975) 50.
[25] C.S. Becquart, K.M. Decker, C. Domain, J. Ruste, Y. Souffez, J.C. Turbatte, J.C. Van Duysen, Radiat. Eff. 142 (1997) 9.
[26] a C version of CDCMD can be found at http://www.ims.uconn.edu/centers/simul/index.htm#xmd.
[27] M.P. Allen, D.J. Tildesley, Computer Simulation of Liquids, Clarendon, Oxford, 1986.
[28] S.M. Ludwig, D. Farkas, D. Pedraza, S. Schmauder, Modelling Simul. Mater. Sci. Eng. 6 (1998) 19.
[29] M.T. Robinson, Phys. Rev. B 40 (1989) 10717.
[30] M.T. Robinson, Radiat. Eff. 141 (1997) 1.
[31] S.T. Nakagawa, Y. Yamamura, Radiat. Eff. 116 (1991) 21.
[32] G. Molière, Z. Naturforsch. A2 (1947) 133.
[33] M.T. Robinson, K. Dan. Vidensk. Selsk. Mater. Fys. Medd. 43 (1993) 28.
[34] O.S. Oen, M.T. Robinson, Nucl. Instrum. and Meth. 132 (1976) 647.
[35] J. Lindhard, M. Scharff, H.E. Schiøtt, K. Dan. Vidensk. Selsk. Mater. Fys. Medd. 33 (14) (1963).
[36] M. Hou, Phys. Rev. A 39 (6) (1989) 2817.
[37] G. Leibfried, in: Bestrahlungseffekte in Festkörpern, Teubner, Stuttgart, 1965.
[38] R. Stoller, A.F. Calder, J. Nucl. Mater. 283–287 (2000) 746.
[39] P.G. Lucasson, R.M. Walker, Phys Rev. 127 (2) (1962) 485.
[40] D.J. Bacon, A.F. Calder, J.M. Harder, S.J. Wooding, J. Nucl. Mater. 205 (1993) 52.
[41] F. Maury, M. Biget, P. Vajda, A. Lucasson, P. Lucasson, Phys. Rev. B 14 (1976) 5303.
[42] A. Scholtz, C. Lehmann, Phys. Rev. B 6 (1972) 813.
[43] A.F. Calder, D.J. Bacon, J. Nucl. Mater. 207 (1993) 25.
[44] C.S. Becquart, M. Hou, A. Souidi, Mater. Res. Soc. Symp. 650 (2001) in press.
[45] J. Dural, J. Ardonceau, J.C. Roussett, J. Phys. (Paris) 38 (1977) 1007.
[46] R.E. Stoller, G.R. Odette, B.D. Wirth, J. Nucl. Mater. 251 (1997) 49.
[47] J.A. Brinkman, Am. J. Phys. 24 (1956) 246.
[48] P. Bergé, Y. Pomeau, C. Vidal (Eds.), L'ordre dans le Chaos, Hermann, éditeurs des Sciences et des Arts, Paris, 1988.
[49] R.Z. Sagdeev, D.A. Usikov, G.M. Zaslavsky, Nonlinear Physics, Harwood Academic, Chur, 1988.
[50] Bacon, Calder, Gao, Radiat. Eff. 141 (1997) 285.